IEICE TRANS. COMMUN., VOL.E88–B, NO.1 JANUARY 2005

PAPER

FDTD Simulation of Shielding Effectiveness of Metal-Coated Plastics for Pulsed Electromagnetic Fields

Jianqing WANG[†a)], **Tetsuji TSUCHIKAWA**[†], ***and*** **Osamu FUJIWARA**[†], ***Members***

SUMMARY The use of metal-coated plastics is increasing as shielding materials of electronic and information products due to their lightweight. In this paper, a finite-difference time-domain (FDTD) algorithm, based on the derivation of a time-domain representation of the surface impedance of an equivalent resistive film, was developed to analyze the electromagnetic penetration of pulsed electromagnetic fields through metal-coated plastics. The validity of the proposed algorithm, in both the far-field and near-field cases, was verified by comparing the calculated penetrated electromagnetic fields or shielding effectiveness with theoretical and measured ones. Good agreement between them demonstrated the usefulness of the FDTD algorithm.

key words: *shielding, pulsed electromagnetic field, metal-coated plastic, FDTD method*

1. Introduction

With the increasing requirement of lightweight for electronic and information products, metal-coated or metal-plated plastics are being widely used as shielding materials [1]. When the metal layer is thinner than its skin depth, however, the electromagnetic (EM) wave penetration is not negligible. On the other hand, as a powerful tool to analyze the shielding effectiveness the finite-difference time-domain (FDTD) method [2] is a convenient means. With the FDTD method, many efforts have been made to model thin metal layers [3]–[5] because the FDTD method suffers from the requirement of fine discretization which would yield a considerable burden on the computation time and memory. This becomes especially difficult for a multi-layer structure [6], [7] such as the metal-coated plastics. To cope with this problem, an approach with a transmission line model was made in [8], in which the transmission coefficient of the multi-layer structure was approximately derived and was replaced with that of an infinitely thin resistive film being formulated via its surface impedance in the FDTD method. This approach was reported to be superior to that in [6] for a multi-layer structure. In this approach, however, the equivalent surface impedance of the resistive film becomes a function of frequency. This means that it cannot be incorporated directly into the conventional FDTD algorithm for an EM pulse excitation. In this paper, based on the above approach, an FDTD algorithm is newly developed to analyze the shielding effectiveness of metal-coated plastics for a pulse excitation. This is realized via the derivation of a time-domain representation of the surface impedance of an equivalent resistive film with the fast Fourier transformation (FFT). The validity of the FDTD algorithm is verified via comparing its numerical results with the theoretical and experimental ones.

Manuscript received April 14, 2004.
Manuscript revised July 26, 2004.

[†]The authors are with the Department of Computer Science and Engineering, Graduate School of Engineering, Nagoya Institute of Technology, Nagoya-shi, 466-8555 Japan.
a) E-mail: wang@elcom.nitech.ac.jp

2. Equivalent Resistive Film

Figure 1 shows a model of metal-coated plastics with a multi-layer structure. The model is assumed to spread infinitely in the x-y plane. For any incident EM waves that impinge on the material with an incident angle θ_i, the fields would propagate with an angle θ_t from the z-axis. Due to the high conductivity of the metal layer compared to that of air, the transmission angle θ_t can be approximated by θ_t=0. This means that the penetration of the tangential field components inside the metal-coated plastics can be modeled by a plane wave propagating in the z direction or a one-dimensional transmission line model. According to [8], the multi-layer structure can be replaced with an infinitely thin resistive film which has the same transmission coefficient as itself. This yields an equivalent surface impedance $Z_s(f)$ for the multi-layer structure, which is given by

$$Z_s(f) = \frac{T(f)}{2[1 - T(f)]} \times \eta_0 \tag{1}$$

where $T(f)$ is the transmission coefficient approximately derived from the one -dimensional transmission line model of the multi-layer structure and η_0 is the free-space intrinsic impedance.

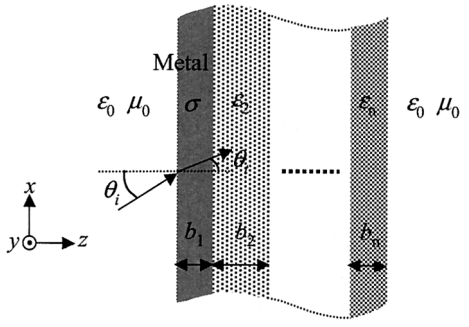

Fig. 1 Model of multi-layer structure.

3. FDTD Algorithm

Figure 2 shows an FDTD grid for an equivalent thin resistive film of the multi-layer structure. From the boundary condition we have

$$\hat{z} \times (H^+ - H^-) = \frac{E_s}{Z_s(f)} \tag{2}$$

in the frequency domain where E_s is the electric field along the resistive film surface, which yields

$$E_x\left(i+\frac{1}{2}, j, k\right) = Z_s(f) \left[H_y(i+\frac{1}{2}, j, k-\frac{1}{2}) - H_y\left(i+\frac{1}{2}, j, k+\frac{1}{2}\right)\right], \tag{3}$$

$$E_y\left(i, j+\frac{1}{2}, k\right) = Z_s(f) \left[H_x\left(i, j+\frac{1}{2}, k+\frac{1}{2}\right) - H_x\left(i, j+\frac{1}{2}, k-\frac{1}{2}\right)\right]. \tag{4}$$

In order to simulate the EM penetration of pulsed electromagnetic fields and the shielding effectiveness in a broad frequency band, we employed a time domain representation $z_s(t)$ of $Z_s(f)$ in the FDTD algorithm, which is calculated from the inverse FFT of $Z_s(f)$. On the assumption that the corresponding frequency for the kth frequency data point is $k \times \Delta f$ where Δf is the frequency discretization increment, the frequency data are extended to 2N by conjugating the first N data in order to get a real time response, i.e.,

$$Z_s(k\Delta f) = Z_s^*[(2N+1-k)\Delta f], k = N+1, \ldots, 2N. \tag{5}$$

We thus have

$$z_s^m = z_s[m\Delta t] = \frac{1}{2N\Delta t} \sum_{k=0}^{2N-1} Z_s(k/2N\Delta t) e^{j2\pi km/2N} \times \eta_0 \tag{6}$$

where Δt is the time step equal to $1/(2N\Delta f)$ and only the first N time-domain data are employed in the FDTD implementation.

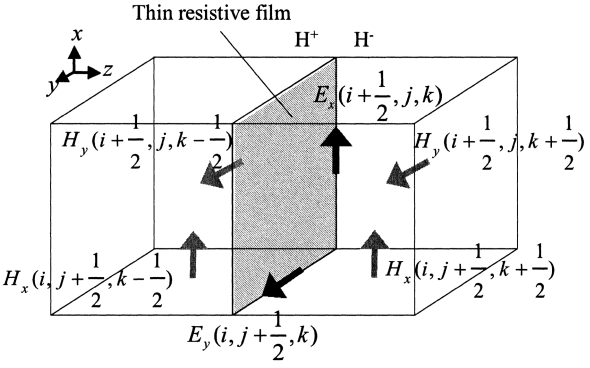

Fig. 2 Arrangement of electric and magnetic fields in the FDTD grid around an equivalent thin resistive film of the metal-coating plastics.

Transforming Eqs. (3) and (4) into the time domain via the discrete convolution formula, we have the following equations for the x and y components of the electric fields at the equivalent resistive film:

$$E_x^n\left(i+\frac{1}{2}, j, k\right) = \sum_{m=1}^{n} z_s^m \Delta t \cdot \left[H_y^{n-m+1}\left(i+\frac{1}{2}, j, k-\frac{1}{2}\right) - H_y^{n-m+1}\left(i+\frac{1}{2}, j, k+\frac{1}{2}\right)\right], \tag{7}$$

$$E_y^n\left(i, j+\frac{1}{2}, k\right) = \sum_{m=1}^{n} z_s^m \Delta t \cdot \left[H_x^{n-m+1}\left(i, j+\frac{1}{2}, k+\frac{1}{2}\right) - H_x^{n-m+1}\left(i, j+\frac{1}{2}, k-\frac{1}{2}\right)\right]. \tag{8}$$

Substituting Eqs. (7) and (8) into Maxwell Equation (Faraday law) in the time domain and rearranging them for the x components of the magnetic fields at the both sides of the equivalent resistive film, we have Eqs. (9) and (10) of the next page.

Similarly, the y components of the magnetic fields are also given in the above form. In such a way the frequency-dependent surface impedance is incorporated into the FDTD algorithm via the neighbor magnetic fields at the both sides of the resistive film.

As can be seen in Eqs. (9) and (10), however, all the past H_x and H_y in the time domain have to be stored at the both sides of the resistive film, which yields an additional burden in memory. Although a solution to this problem is known to derive a recursive convolution scheme by expressing the equivalent impedance z_s^m in exponential functions using Prony approximation, as described in [9], direct implementation of Eqs. (9) and (10) is addopted in this paper to avoid additional calculation burden for the determination of coefficients in Prony approximation.

4. Theoretical Validation

The validity of the FDTD algorithm was verified theoretically for the metal-coated plastic that was assumed to have a two-layer structure. As shown in Fig. 1, the metallic layer had a conductivity (σ) of 5.8×10^7 S/m and a thickness of $b_1 = 2\,\mu$m. The plastic had a relative permittivity (ε_r) of 4.0 and a thickness of $b_2 = 1$ mm. From the one-dimensional transmission line model approximation, $Z_s(f)$ was first derived from Eq. (1) and then its time-domain representation $z_s(t)$ (z_s^m) was determined via the inverse FFT, which was shown in Fig. 3. In the FDTD calculation, the cell size and time step were set to be 2 mm and 3.81 ps, respectively. Twelve perfectly matched layers [2] were employed to absorb the outgoing scattered waves.

Figure 4(a) shows a far-field model. A Gaussian pulsed electric field with an amplitude of 1 V/m was used as an incident field propagating in the z direction. The FDTD algorithm was therefore simplified to the one-dimensional case. Figure 4(b) shows the FDTD-calculated electric field penetrated through the metal-coated plastic, which exhibits ex-

$$
\begin{aligned}
&H_x^{n+\frac{1}{2}}(i, j+\tfrac{1}{2}, k+\tfrac{1}{2}) \\
&= \frac{1}{1+\frac{z_s^1 \Delta t}{\mu \Delta z}} H_x^{n-\frac{1}{2}}(i, j+\tfrac{1}{2}, k+\tfrac{1}{2}) + \frac{\frac{z_s^1 \Delta t}{\mu \Delta z}}{1+\frac{z_s^1 \Delta t}{\mu \Delta z}} H_x^{n-\frac{1}{2}}(i, j+\tfrac{1}{2}, k-\tfrac{1}{2}) \\
&- \frac{\frac{\Delta t}{2\mu \Delta z}}{1+\frac{z_s^1 \Delta t}{\mu \Delta z}} \sum_{m=2}^{n} z_s^m \left[H_x^{n+\frac{1}{2}-m+1}(i, j+\tfrac{1}{2}, k+\tfrac{1}{2}) + H_x^{n-\frac{1}{2}-m+1}(i, j+\tfrac{1}{2}, k+\tfrac{1}{2}) - H_x^{n+\frac{1}{2}-m+1}(i, j+\tfrac{1}{2}, k-\tfrac{1}{2}) - H_x^{n-\frac{1}{2}-m+1}(i, j+\tfrac{1}{2}, k-\tfrac{1}{2}) \right] \\
&+ \frac{(1+\frac{z_s^1 \Delta t}{2\mu \Delta z}) \frac{\Delta t}{\mu \Delta z}}{1+\frac{z_s^1 \Delta t}{\mu \Delta z}} E_y^n(i, j+\tfrac{1}{2}, k+1) - \frac{(\frac{\Delta t}{\mu \Delta z})^2 \frac{z_s^1}{2}}{1+\frac{z_s^1 \Delta t}{\mu \Delta z}} E_y^n(i, j+\tfrac{1}{2}, k-1) - \frac{(1+\frac{z_s^1 \Delta t}{2\mu \Delta z}) \frac{\Delta t}{\mu \Delta y}}{1+\frac{z_s^1 \Delta t}{\mu \Delta z}} \left[E_z^n(i, j+1, k+\tfrac{1}{2}) - E_z^n(i, j, k+\tfrac{1}{2}) \right] \\
&- \frac{\frac{z_s^1 \Delta t}{2\mu \Delta z} \frac{\Delta t}{\mu \Delta y}}{1+\frac{z_s^1 \Delta t}{\mu \Delta z}} \left[E_z^n(i, j+1, k-\tfrac{1}{2}) - E_z^n(i, j, k-\tfrac{1}{2}) \right], \qquad (9)
\end{aligned}
$$

$$
\begin{aligned}
&H_x^{n+\frac{1}{2}}(i, j+\tfrac{1}{2}, k-\tfrac{1}{2}) \\
&= \frac{1}{1+\frac{z_s^1 \Delta t}{\mu \Delta z}} H_x^{n-\frac{1}{2}}(i, j+\tfrac{1}{2}, k-\tfrac{1}{2}) + \frac{\frac{z_s^1 \Delta t}{\mu \Delta z}}{1+\frac{z_s^1 \Delta t}{\mu \Delta z}} H_x^{n-\frac{1}{2}}(i, j+\tfrac{1}{2}, k+\tfrac{1}{2}) \\
&+ \frac{\frac{\Delta t}{2\mu \Delta z}}{1+\frac{z_s^1 \Delta t}{\mu \Delta z}} \sum_{m=2}^{n} z_s^m \left[H_x^{n+\frac{1}{2}-m+1}(i, j+\tfrac{1}{2}, k+\tfrac{1}{2}) + H_x^{n-\frac{1}{2}-m+1}(i, j+\tfrac{1}{2}, k+\tfrac{1}{2}) - H_x^{n+\frac{1}{2}-m+1}(i, j+\tfrac{1}{2}, k-\tfrac{1}{2}) - H_x^{n-\frac{1}{2}-m+1}(i, j+\tfrac{1}{2}, k-\tfrac{1}{2}) \right] \\
&- \frac{(1+\frac{z_s^1 \Delta t}{2\mu \Delta z}) \frac{\Delta t}{\mu \Delta z}}{1+\frac{z_s^1 \Delta t}{\mu \Delta z}} E_y^n(i, j+\tfrac{1}{2}, k-1) + \frac{(\frac{\Delta t}{\mu \Delta z})^2 \frac{z_s^1}{2}}{1+\frac{z_s^1 \Delta t}{\mu \Delta z}} E_y^n(i, j+\tfrac{1}{2}, k+1) - \frac{(1+\frac{z_s^1 \Delta t}{2\mu \Delta z}) \frac{\Delta t}{\mu \Delta y}}{1+\frac{z_s^1 \Delta t}{\mu \Delta z}} \left[E_z^n(i, j+1, k-\tfrac{1}{2}) - E_z^n(i, j, k-\tfrac{1}{2}) \right] \\
&- \frac{\frac{z_s^1 \Delta t}{2\mu \Delta z} \frac{\Delta t}{\mu \Delta y}}{1+\frac{z_s^1 \Delta t}{\mu \Delta z}} \left[E_z^n(i, j+1, k+\tfrac{1}{2}) - E_z^n(i, j, k+\tfrac{1}{2}) \right]. \qquad (10)
\end{aligned}
$$

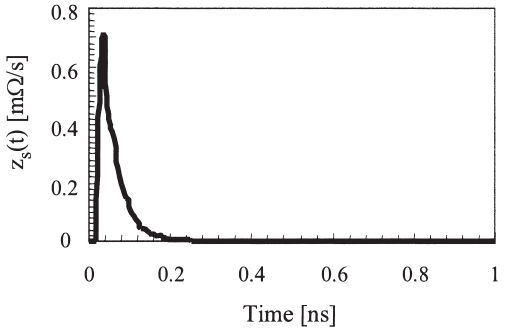

Fig. 3 Time domain representation $z_s(t)$ of the equivalent surface impedance $Z_s(f)$.

cellent agreement with the result from the transmission line theory. This demonstrated the validity of the FDTD algorithm for a plane wave incidence with the electric field components parallel to the metal surface.

Figure 5(a) shows a near-field model with an electric dipole. In this case, due to the difficulty in deriving a theoretical representation for the multi-layer structure, one metallic layer structure was used. The electric dipole had a length of 1 cm and was placed at a distance of d_1 from the metal surface. The dipole was excited with a Gaussian pulsed voltage source whose peak voltage was 1 kV. The electric field that penetrated to the other side of the metal surface was calculated with the FDTD algorithm at an observation point with a distance of d_2 from the metal surface. Figs. 5(b) and (c) show the penetrated electric field at some specified distances from the metal. Also shown in the figure are the theoretical values that were derived from an electric dipole moment for an electrically thin metal sheet. According to [10], the penetrated electric field in the frequency domain is theoretically given as

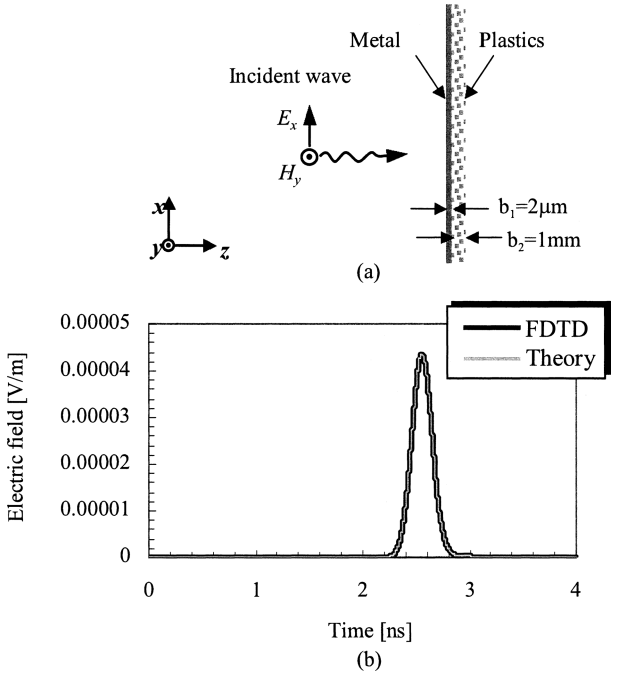

Fig. 4 Electric field penetrated through an infinitely large metal-coating plastic sheet for a plane wave incidence.

$$
\begin{aligned}
E_x = &\frac{I_0 lk}{2\pi j \omega \varepsilon_0} \\
&\int_0^\infty \left[-\left(\gamma_0^2 + \frac{u^2}{2} \right) A + \frac{u}{2} \alpha_1 B \right] e^{-\alpha_1 (d_1 + d_2)} du \qquad (11)
\end{aligned}
$$

where

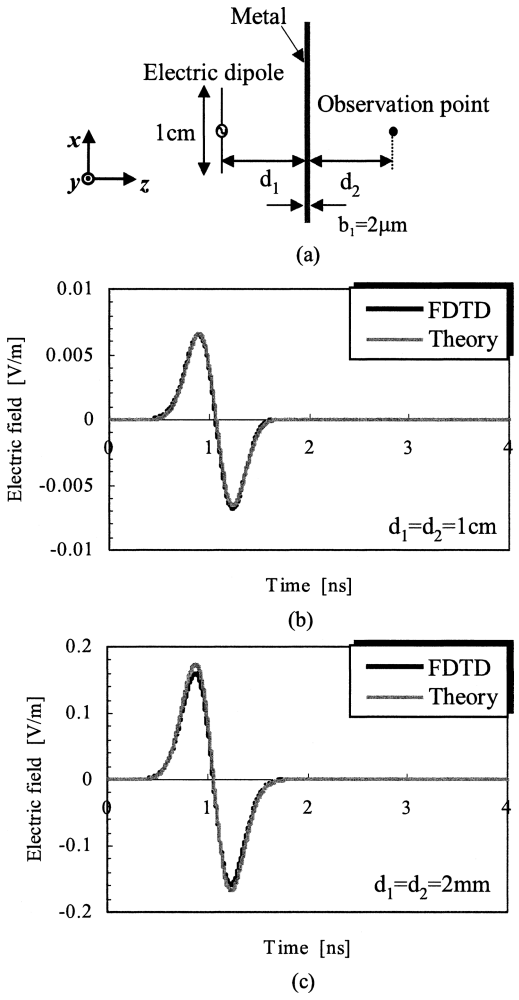

Fig. 5 Electric field penetrated a sufficiently large metal sheet for an electric dipole incidence. (a) Model, (b) electric field waveform when $d_1 = d_2 = 1$ cm, (c) electric field waveform when $d_1 = d_2 = 2$ mm.

$$A = \frac{\chi\alpha(u/\alpha_1)}{\chi^2 + (k\alpha)^2 \sinh(\alpha_2 b_1) + 2\chi k\alpha \cosh(\alpha_2 b_1)}$$

$$B = \frac{\alpha(\chi - 1)(k^2 - \chi)(u/\alpha_1)^2}{(k^2 + \alpha^2)\sinh(\alpha_2 b_1) + 2k\alpha \cosh(\alpha_2 b_1)} \cdot \frac{\sinh(\alpha_2 b_1)}{(k^2\alpha^2 + \chi^2)\sinh(\alpha_2 b_1) + 2k\alpha\chi \cosh(\alpha_2 b_1)}$$

$$\alpha_1 = \sqrt{u^2 + \gamma_0^2}, \alpha_2 = \sqrt{u^2 + \gamma^2}, \alpha = \alpha_2/\alpha_1$$

$$\gamma_0^2 = j\omega\mu_0 \cdot j\omega\varepsilon_0, \gamma^2 = j\omega\mu\sigma, \chi = \gamma^2/\gamma_0^2$$

and I_0 is the dipole moment current, l is the dipole length and k is the wave-number. Moreover, γ_0 and γ denote the propagation constants in free space and in the metal sheet, respectively. The dipole current I_0 was obtained from the average of the FDTD-calculated currents along the dipole moment, which was found to have a dominant component around 1 GHz from the FFT. Substituting the current into Eq. (11) gave the theoretical electric field penetration in the frequency domain. Its waveform in the time domain was then derived from the inverse FFT. From Fig. 5, Good agreement was found between the FDTD-calculated and the theoretical results when $d_1 = d_2 = 1$ cm. With the distance approaching to 2 mm both for d_1 and d_2, however, some discrepancies were observed. The discrepancies seem to be due to the inclined incident field components that cannot be ignored. To examine the effectiveness of the one-dimensional transmission line approximation in the near-field case, the errors between the FDTD-calculated and the theoretical results were investigated for the penetrated electric fields at the dominant frequency (1 GHz) of the dipole current. The result is shown in Fig. 6. It was found that when the distance d_1 or d_2 reduced to 2 mm (1/150 wavelength), a relative error of 13% from the theoretical value was observed for the penetrated electric fields. It should be noted, however, that as long as the distances of both d_1 and d_2 are larger than 1 cm (1/30 wavelength) to the metal surface, the FDTD-calculated results have an accuracy within 10%.

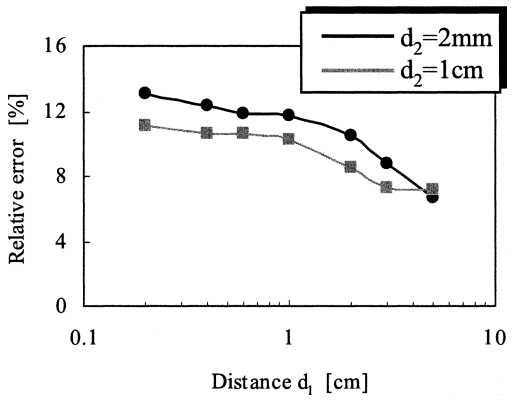

Fig. 6 Relative errors of penetrated electric field between FDTD-calculated and theoretical values.

5. Experimental Validation

The FDTD algorithm was also validated experimentally in the frequency domain in a full anechoic chamber. As shown in Fig. 7, a commercially available metal-coated plastic sheet with a four-layer structure was used in the experiment. A loop antenna with a radius of 0.5 cm was excited using a sweeping signal generator, and the penetrated electric fields were observed at a distance of 1 cm from the sheet using another loop antenna (radius: 0.5 cm) connected to a spectrum analyzer via a semi-rigid cable (outside diameter: 1 mm). The sheet size was 180 cm × 120 cm which was large enough compared to the antenna size and its distance to the sheet. The spacing of the probe from the plastic sheet was set by placing a wood board 1 cm thick between the probe and the sheet and then extracted it during the measurement. The alignment of the transmitting loop antenna and the probe was made by marking the center of two sides of the plastic sheet. The position error in experimental setting was less than 1 mm, which yielded an error in the measured magnetic fields up to 0.5 dB at maximum according to our simulation results.

To obtain the shielding effectiveness in the frequency

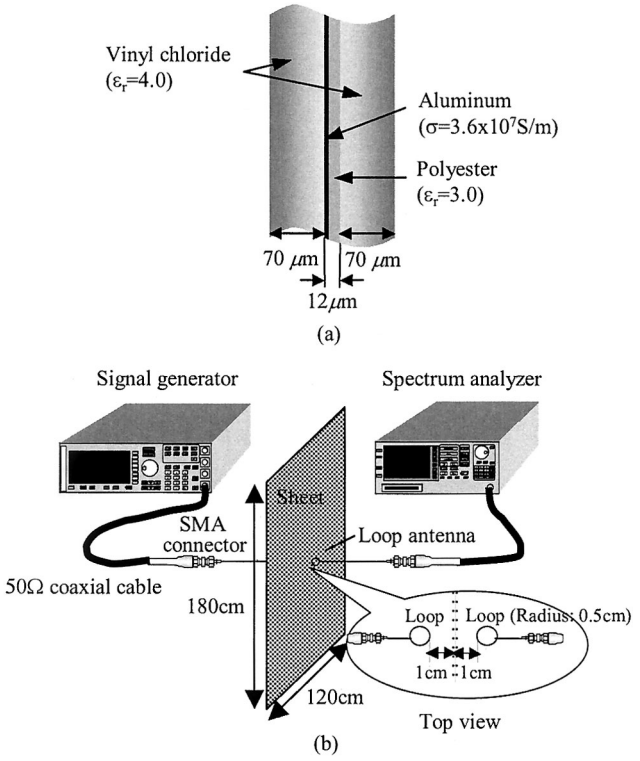

Fig. 7 (a) Structure of metal-coating plastic sheet, and (b) experimental layout.

domain, the magnetic field $H_{y0}(f)$ in the absence of the metal-coated plastic sheet and $H_y(f)$ in the presence of the sheet were measured, and then the magnetic field shielding effectiveness SE was derived as

$$SE = 20\log_{10}\left|\frac{H_{y0}(f)}{H_y(f)}\right|. \tag{12}$$

On the other hand, in the FDTD calculation, the magnetic field $H_{y0}(t)$ in the absence of the metal-coated plastic sheet and $H_y(t)$ in the presence of the sheet were calculated, and then were transformed to the frequency domain using the FFT, respectively, to obtain $H_{y0}(f)$ and $H_y(f)$. The magnetic field shielding effectiveness was then derived from Eq. (12).

A problem in the FDTD calculation was that the accurate thickness of the aluminum-coating layer was not provided in the catalogue of the sheet. It was only given that the thickness ranges from 0.01 to 0.04 μm, and the limitation to see through the sheet is 0.03 μm. Since the sheet considered was completely opaque, we assumed the thickness of the aluminum-coated layer to be 0.04 μm in the FDTD calculation. Figure 8 shows the FDTD-calculated shielding effectiveness in thick solid-line and the measured shielding effectiveness in diamonds as a function of frequency. As can be seen, the calculated result was in fair agreement with measurement from 0.1 to 1 GHz. The maximum difference between them was smaller than 2 dB except for 800 MHz. With changing the thickness of the aluminum-coating layer from 0.03 μm to 0.05 μm, as also shown in Fig. 8, the FDTD-calculated shielding effectiveness shifted from the thin dash-line to the thin solid-line. It showed that a difference of 0.01 μm on the aluminum-coated layer yielded a variation of the shielding effectiveness about 2 dB, and the 0.05-μm thick aluminum-coated layer gave a shielding effectiveness closer to the measurement. These results assured the usefulness of the FDTD algorithm in simulating the EM penetration and shielding effectiveness of pulsed EM fields. As for the 4 dB lower shielding effectiveness at 800 MHz in the measurement compared to the FDTD calculation, it should be attributed to a measurement uncertainty. In the absence of the metal-coated plastic sheet, the frequency characteristics of the measured magnetic field were almost flat, while they exhibited a small peak around 800 MHz in the presence of the sheet. This resulted in the lower shielding effectiveness.

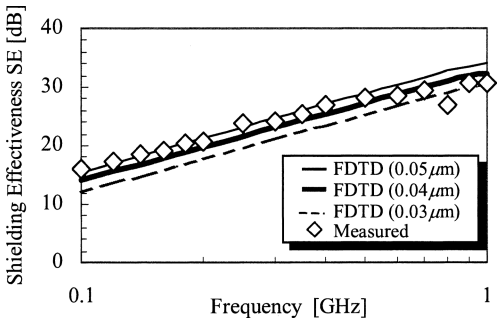

Fig. 8 FDTD-calculated and measured magnetic field shielding effectiveness versus frequency.

6. Conclusion

An FDTD algorithm has been developed to analyze the electromagnetic penetration and shielding effectiveness of metal-coated plastics for pulsed EM fields. By replacing the metal-coated plastics with an infinitely thin resistive film that has the same transmission coefficient, a frequency-dependent surface resistance of the resistive film has been derived and its time-domain representation via the inverse FFT has been incorporated into the FDTD algorithm. The FDTD algorithm has been applied to analyze the penetration of pulsed EM fields and shielding effectiveness in a broad frequency band in both the far and near-field cases. The results have been found to be in good agreement with theoretical or measured ones even in the near field case as long as the distances of the excitation and observation points are larger than 1 cm (or 1/30 wavelength) from the shielding material. Moreover, with the aid of a pluse excitation and the FFT technique, one can provide the frequency characteristics of shielding effectiveness just from one FDTD run, although somewhat additional memory is needed for the convolution in time domain.

The future subject is to improve the FDTD simulation accuracy for inclined EM incidence.

References

[1] M.S. Sarto, S.D. Michele, P. Leerkamp, and H. Thuis, "An innova-

tive shielding concept for EMI reduction," IEEE EMC Newsletter, no.190, pp.22–28, 2001.

[2] A. Taflove, Computational Electrodynamics: The Finite-Difference Time-Domain Method, Artech House, Norwood, MA, 1995.

[3] J.G. Maloney and G.S. Smith, "A comparison of methods for modeling electrically thin dielectric and conducting sheets in the finite-difference time-domain (FDTD) method," IEEE Trans. Antennas Propag., vol.41, no.5, pp.690–694, May 1993.

[4] S. Van den Berghe, F. Olyslager, and D. De Zutter, "Accurate modeling of thin conducting layers in FDTD," IEEE Microw. Guid. Wave Lett., vol.8, no.2, pp.75–77, Feb. 1998.

[5] M. Feliziani, F. Maradei, and G. Tribellini, "Field analysis of penetrable conductive shields by the finite-difference time-domain method with impedance network boundary conditions (INBC's)," IEEE Trans. Electromagn. Compat., vol.41, no.4, pp.307–319, Nov. 1999.

[6] C.J. Railton and J.P. McGeehan, "An analysis of microstrip with rectangular and trapezoidal conductor cross sections," IEEE Trans. Microw. Theory Tech., vol.38, no.8, pp.1017–1022, Aug. 1990.

[7] M.S. Sarto, "A new model for the FDTD analysis of the shielding performances of thin composite structure," IEEE Trans. Electromagn. Compat., vol.41, no.4, pp.298–306, Nov. 1999.

[8] T. Fukazawa, H. Ohmine, I. Chiba, and Y. Sunahara, "Simulation of transmission waves through multi layered thin conducting sheets by FDTD method," IEICE Trans. Commun. (Japanese Edition), vol.J83-B, no.5, pp.711–719, May 2000.

[9] K.S. Kunz and R.J. Luebbers, The Finite Difference Time Domain Method for Electromagnetics, Chapter 9, CRC Press, Boca Raton, FL, 1993.

[10] T. Yamaguchi, Y. Okumura, and Y. Amemiya, "The relation between the near-field and the far-field shielding effectiveness for the plane sheet," IEICE Trans. Commun. (Japanese Edition), vol.J74-B-II, no.2, pp.79–82, Feb. 1991.

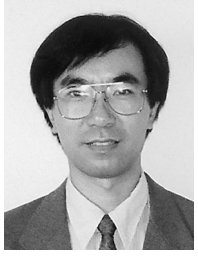

Jianqing Wang received the B.E. degree in electronic engineering from Beijing Institute of Technology, Beijing, China, in 1984, and the M.E. and D.E. degrees in electrical and communication engineering from Tohoku University, Sendai, Japan, in 1988 and 1991, respectively. He was a Research Associate with Tohoku University and a Senior Engineer with Sophia Systems Co., Ltd., prior to joining the Department of Electrical and Computer Engineering, Nagoya Institute of Technology, Nagoya, Japan, in 1997, where he is currently an Associate Professor. His research interests include electromagnetic compatibility, bioelectromagnetics and digital communications.

Tetsuji Tsuchikawa received the B.E. and M.E. degrees in electrical and computer engineering from Nagoya Institute of Technology, Japan, in 2000 and 2002, respectively. He is currently with Aisin AW Co. Ltd.

Osamu Fujiwara received the B.E. degree in electronic engineering from Nagoya Institute of Technology, Nagoya, Japan, in 1971, and the M.E. and the D.E. degrees in electrical engineering from Nagoya University, Nagoya, Japan, in 1973 and in 1980, respectively. From 1973 to 1976, he worked in the Central Research Laboratory, Hitachi, Ltd., Kokubunji, Japan, where he was engaged in research and development of system packaging designs for computers. From 1980 to 1984 he was with the Department of Electrical Engineering, Nagoya University. In 1984 he joined the Department of Electrical and Computer Engineering, Nagoya Institute of Technology, where he is currently a professor. His research interests include measurement and control of electromagnetic interference due to discharge, bioelectromagnetics, and other related areas of electromagnetic compatibility. Dr. Fujiwara is a member of the Institute of Electrical Engineers of Japan, and the Institute of Electrical and Electronic Engineers (IEEE).